Journal of Applied Polymer Science

Curing and Thermal Behaviors of Inorganic–Organic Hybrid Polyarylacetylene Resins with Polyhedral Oligomeric Octa(propargylaminophenyl)silsesquioxane

Haibo Fan, Xiangmei Li, Yanlin Liu, Rongjie Yang

School of Materials Science and Engineering, National Laboratory of Flame Retardant Materials, Engineering Research Center of Fire-Safe Materials and Technology, Ministry of Education, Beijing Institute of Technology, Haidian District, Beijing 100081, People's Republic of China

Correspondence to: X. Li (E-mail: bjlglxm@bit.edu.cn)

ABSTRACT: Polyhedral oligomeric octa(propargylaminophenyl)silsesquioxane (OPAPS) was used to prepare composite resins with prepolyarylacetylene (prePAA). The curing and thermal behaviors of the PAA/OPAPS composites were studied through Fourier-transform infrared (FTIR), X-ray diffraction (XRD), differential scanning calorimetric (DSC), thermogravimetric (TGA), and scanning electron microscopic (SEM) analysis and by direct observation. The morphologies of the PAA/OPAPS resins proved that there was good compatibility between PAA and OPAPS. FTIR analysis indicated formation of a conjugated diene and aromatic ring groups in the thermal curing process of the resins. DSC analysis implied that the addition of OPAPS to prePAA could decrease the exothermic heat and widen the temperature range in the curing process of prePAA. According to TGA analysis, a 10 wt % addition of OPAPS to PAA can maintain the thermal stability of PAA in N_2 atmosphere and somewhat enhance the thermal-oxidative stability.
 J. Appl. Polym. Sci. 128: 4361–4367, 2013

KEYWORDS: composites; properties and characterization; resins; thermosets; thermal properties

Received 16 August 2012; accepted 7 October 2012; published online 25 October 2012
DOI: 10.1002/app.38690

INTRODUCTION

Polyarylacetylene (PAA), a new kind of high performance resin, is increasingly being developed as the matrix for high-temperature composites in next-generation carbon–carbon composites, ablation materials, and structural materials owing to its outstanding heat resistance.[1–3] PAA is a highly cross-linked aromatic polymer that contains only carbon and hydrogen when it is cured by means of addition polymerization, as shown in Scheme 1. This addition polymerization improves the thermal stability and oxidation characteristics of PAA. The char yield of the PAA resins can reach approximately 85–90 wt % when they are heated to high temperatures in an inert atmosphere.[4,5]

However, there are still two main shortcomings for PAA resin.[6,7] First, the curing exothermic heat is very high and the curing rate is so fast that the resin could explode during processing. Second, the mechanical properties of PAA composites are comparably poor, especially the interlaminar shear strength, and the composites are brittle and have poor structural integrity. Polymer blending is a traditional method for improving the performance of PAA resins.[8] For example, novolac resins, including propargyl–novolac resin, boron–novolac resin, and *N*-(4-propargyloxyphenyl) maleimide, blended with prePAA could slow the curing rate.[6,9,10] However, the char yield of the modified PAA resins decreases significantly due to the poor thermal stability of the blending polymers.

Polyhedral oligomeric silsesquioxanes (POSSs) are a type of three-dimensional, structurally well-defined cage molecule with the general formula $(RSiO_{1.5})_n$. The inorganic silica-like core is surrounded by organic groups and the cage size is about 1.5 nm.[11–14] Typical POSS derivatives have the structure of a cube-octameric framework covalently bonded with eight organic groups, one or more of which is reactive or polymerizable. These POSS derivatives have attracted considerable interest for many years due to their high performance, which originates from the combination of advantages of the inorganic and organic components in these materials. POSS cages can be incorporated into polymers via copolymerization,[15–18] grafting,[19,20] or blending.[21–23] They have been successfully used to improve polymer properties such as use temperature, oxidation resistance, and mechanical properties.[17,21,22,24,25]

Additional Supporting Information may be found in the online version of this article.

Applied Polymer SCIENCE

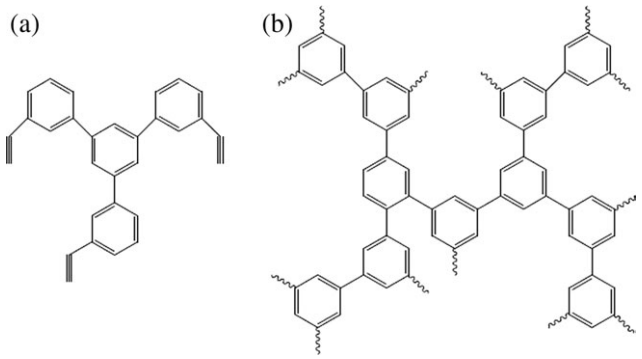

Scheme 1. Molecular structure of (a) prePAA; (b) PAA resin.

In our previous work,[26] a novel polyhedral oligomeric octa(propargylaminophenyl)silsesquioxane (OPAPS, $(SiO_{1.5}C_6H_4NHCH_2C{\equiv}CH)_8$) was prepared from octaphenylsilsesquioxane (OPS) via octa(aminophenyl)silsesquioxane (OAPS) by following the literature methods (Scheme 2).[27–29] The terminal alkynyl groups in OPAPS could participate in the thermal curing process of prePAA. In this study, we investigated the thermal curing reactions of prePAA composites based on OPAPS, and the thermal behaviors of the curing products have been analyzed.

EXPERIMENTAL

Materials

A pre-polyarylacetylene (prePAA) was provided by the Institute of Aerospace Materials and Processing Technology, China. Octaphenylsilsesquioxane [OPS, $Si_8O_{12}(C_6H_5)_8$, M = 1033.2, 97%] was purchased from Hybrid Plastics, USA. Propargyl bromide was obtained from Alfa Aesar, China. Triethylamine, NaCl, Na_2SO_4, and solvents such as dimethyl formamide (DMF), tetrahydrofuran (THF), ethyl acetate, and hexane, were of analytical purity and obtained from Beijing Chemical Works, China.

Synthesis of OAPS

Octa(aminophenyl)silsesquioxane (OAPS) was synthesized from OPS by the method described in the literature.[27–29] OAPS: ^{1}H-nuclear magnetic resonance (NMR) spectroscopy (500 MHz, DMSO-d_6, δ): 7.4–6.2 (2.0H, Ar H), 5.4–4.5 (1.0H, –NH_2); ^{29}Si solid NMR (400 MHz, δ): −68.3, −77.5; ^{13}C-NMR (500 MHz, DMSO-d_6, δ): 153.2, 147.9, 135.1, 131.4, 128.6, 121.2, 119.3, 116.4, 114.6, 113.3; Fourier transform-infrared (FTIR) spectroscopy (KBr): ν = 3456 and 3358 (-NH_2), 1115 (Si—O) cm^{-1}; Analysis calculated for OAPS: C 50. 0, H 4.16, N 9.71; found: C 48.9, H 4.38, N 9.31.

Synthesis of OPAPS

Octa(propargylaminophenyl)silsesquioxane (OPAPS) was synthesized from OAPS by our previously reported method.[26] The

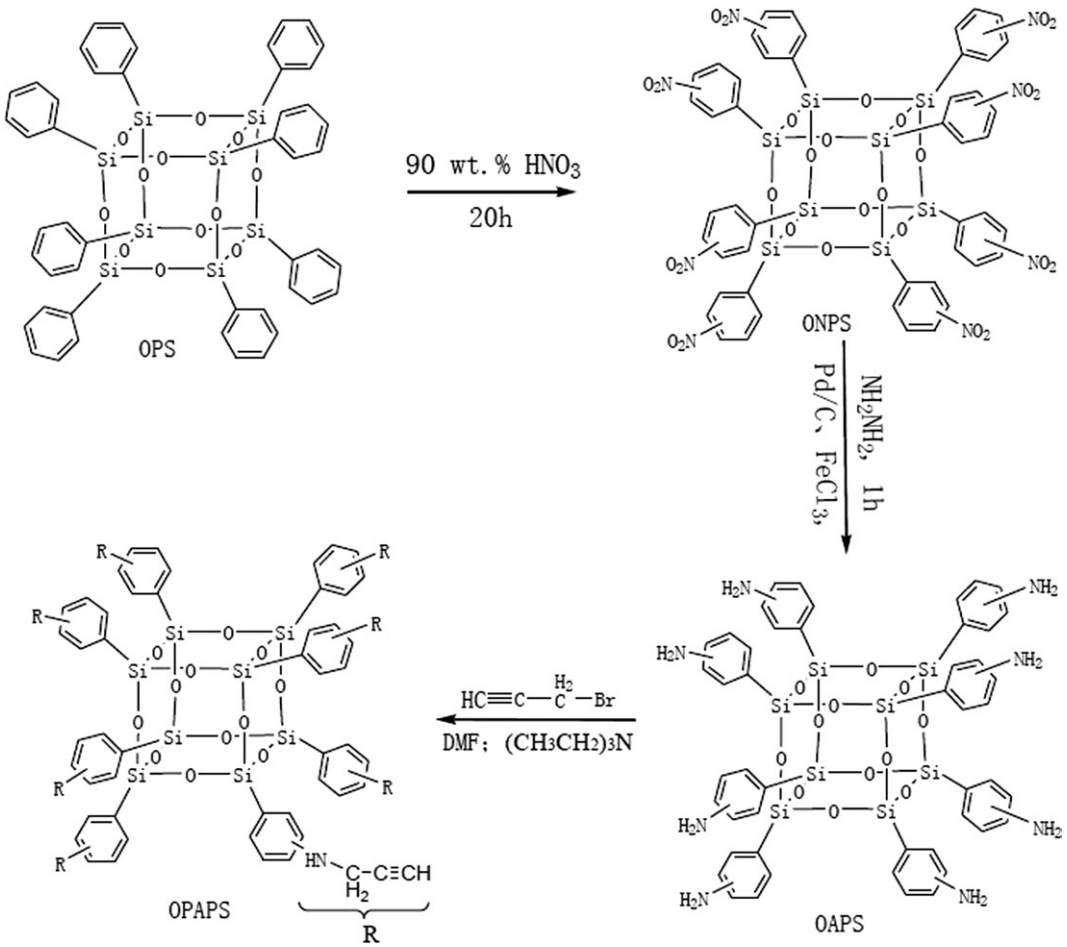

Scheme 2. Synthesis of OPAPS.

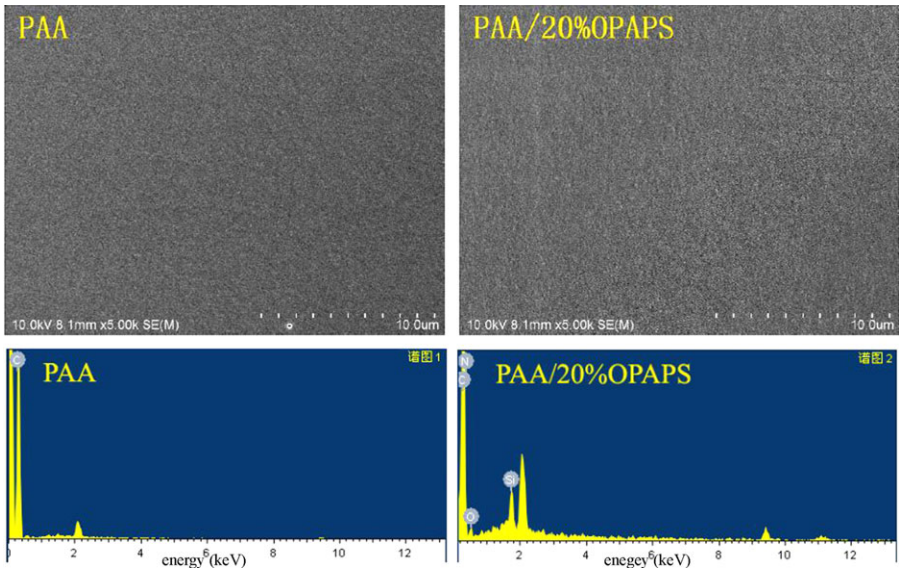

Figure 1. SEM micrographs and EDXS spectra of PAA and PAA/20%OPAPS. [Color figure can be viewed in the online issue, which is available at wileyonlinelibrary.com.]

detail process of synthesis of OPAPS could be found in the Supporting Information. OAPS: ^{1}H-NMR (500 MHz, DMSO-d_6, δ): 7.9–6.5 (3.81H, Ar H), 4.2–4.0 (0.54H, –NH–), 4.0–3.5 (1.84H, –CH_2–), 3.1–2.8 (1.00H, –C≡CH); ^{29}Si solid NMR (400 MHz, δ): −77.9; ^{13}C-NMR (500 MHz, DMSO-d_6, δ): 162.4, 146.9, 128.9, 124.3, 120.0, 79.5, 75.1; FTIR (KBr): 3288, 2113, and 642 (–C≡CH), 3375 (–NH–), 2922, and 2827 (–CH_2–), 1115 (Si—O) cm^{-1}; Analysis calculated for OPAPS: C 59.2, H 4.39, N 7.68; found: C 56.1, H 4.43, N 7.69.

Thermal Curing of PAA Composites Based on OPAPS

Three different concentrations (10, 20, and 30 wt %) of the OPAPS blending with prePAA have been looked at in this work. The OPAPS powder was weighed and dissolved in THF. PrePAA was then added to the solution and stirred to obtain a homogeneous solution at room temperature. The solution was heated to 40°C with continuous stirring to evaporate the solvent and then degassed under vacuum at 40°C for 15 min to remove the residual solvent. The viscous prePAA/OPAPS (2 g) mixture was then transferred to a glass bottle. The resins were heated to obtain thermally cured products under air in an oven with a continuous program of 130°C/1 h → 150°C/1 h → 170°C/1 h → 190°C/1 h → 210°C/1 h →230°C/1 h → 250°C/1 h. The cured PAA/OPAPS composites were black–brown solids.

Characterization

Scanning electron microscopy (SEM) was used to study the morphology of a gold-coated cross-sectional area with an accelerating voltage of 10.0 kV. The C, O, and Si elements in the samples were verified by an energy dispersive X-ray spectroscopy (EDXS EX-350) in the SEM (Hitachi S-4800).

The FTIR spectra of these products pressed into KBr pellets were recorded by a Nicolet 6700 IR spectrometer. The spectra were collected in 32 scans with a spectral resolution of 4 cm^{-1}.

DSC measurements were performed on a Netzsch DSC 204 F1 instrument (Germany) in the temperature range of 30–350°C with a heating rate of 10°C/min in a nitrogen flow of 20 mL/min.

The X-ray diffraction (XRD) analysis was achieved using an XPERT-PRP diffractometer system; Cu Kα radiation was used with a copper target over the 2θ range of 5–60°.

Thermal gravimetric analysis (TGA) was performed on a Netzsch 209 F1 thermal analyzer at a heating rate of 10°C/min over the temperature range of 40–900°C.

RESULTS AND DISCUSSION

Morphological Properties of PAA/OPAPS Composites

The PAA/OPAPS composites with different amounts of OPAPS were prepared. As can be seen from the fractured surfaces of

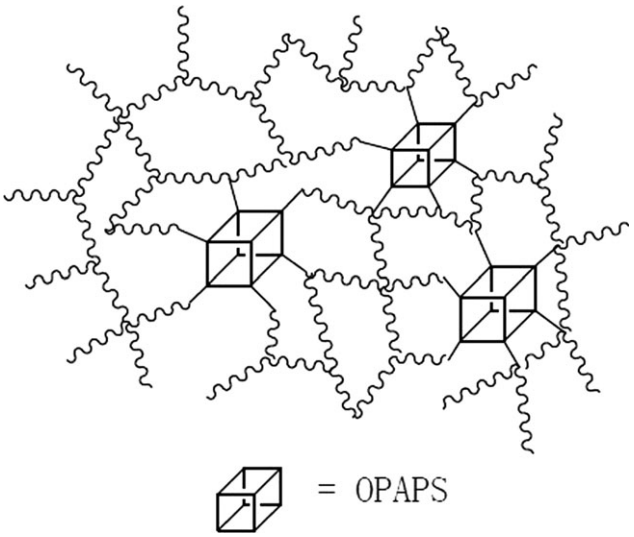

Scheme 3. Structure of PAA/OPAPS composite.

Applied Polymer SCIENCE

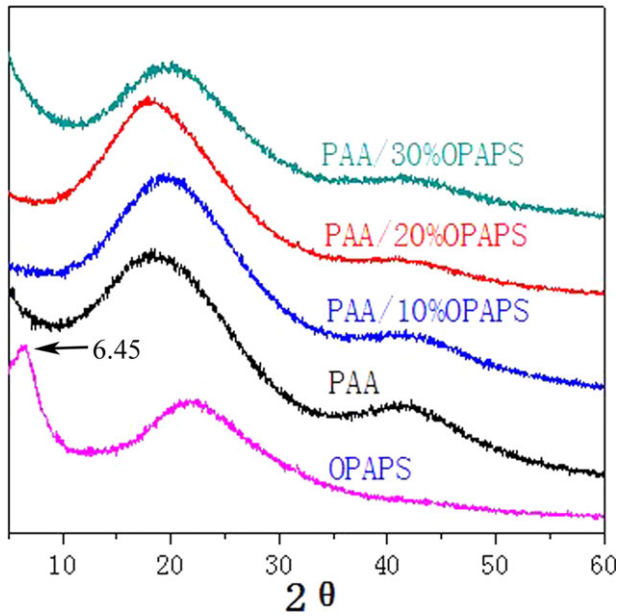

Figure 2. X-ray diffraction patterns of OPAPS, PAA, and PAA/OPAPS. [Color figure can be viewed in the online issue, which is available at wileyonlinelibrary.com.]

the PAA and PAA/OPAPS composites (in the Supporting Information), both the PAA/10%OPAPS and the PAA/20%OPAPS samples have a bright black appearance, the same as the pure PAA sample. However, the PAA/30%OPAPS sample is not very bright because of the high amount of OPAPS. The compatibility between PAA and OPAPS is better compared with PAA/OPS because the PAA/OPS sample phase separates into a polymer rich upper layer and an OPS rich lower layer (in the Supporting Information).

The morphologies of the fractured surfaces and the EDXS spectra of PAA and PAA/20%OPAPS resins were observed by SEM. In Figure 1, it is seen that the PAA/20%OPAPS composite shows homogenous and smooth morphology, with no macro-

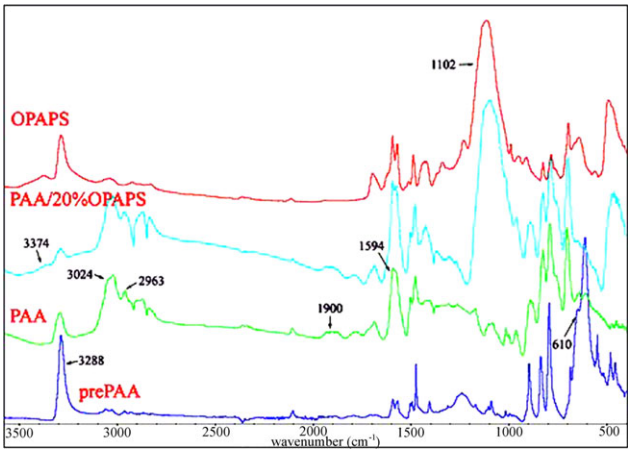

Figure 3. FTIR spectra of prePAA, OPAPS, PAA, and PAA/20%OPAPS. [Color figure can be viewed in the online issue, which is available at wileyonlinelibrary.com.]

Table I. Assignment of FTIR Spectra of prePAA, OPAPS, PAA, and PAA/20%OPAPS

Wavenumber (cm^{-1})	Assignment
3374	—NH— stretching vibration
3288	C—H stretching vibration of —C≡CH
3024	C_{Ar}—H stretching vibration
2963	C—H stretching vibration of —CH=CH—
1900	overtone band of aromatic ring
1594	C=C stretching vibration
1102	Si—O—Si vibration
610	C—H deformation vibration of —C≡CH

phase separation. The Si and O elements are observed in the EDXS spectra of the PAA/20%OPAPS composite. The well-dispersed PAA/20%OPAPS composite can be attributed to reactions among the terminal alkynyl groups of prePAA and OPAPS by which Si—O cages are connected to the cross-linking PAA networks. The compatibility of OPAPS and PAA is enhanced. The structure of the PAA/OPAPS composite is shown in Scheme 3.

XRD Analysis of PAA/OPAPS

The XRD patterns of the OPAPS, PAA, and PAA/OPAPS composites are displayed in Figure 2. PAA or PAA/OPAPS composites show two wide, amorphous diffraction peaks. Compared with PAA/OPAPS, OPAPS shows a diffraction peak at $2\theta = 6.45°$, indicating a *d*-spacing of 13.7 Å (by Bragg's equation). This diffraction peak is related to the local order among OPAPS molecules of Si—O caged structure.[32,33] The cross-linking reactions between PAA and OPAPS have eliminated the local order of the individual OPAPS molecules.

FTIR Analysis of PAA/POSS

Figure 3 presents FTIR curves of prePAA, OPAPS, PAA, and PAA/20%OPAPS, and the assignment of the absorption peaks

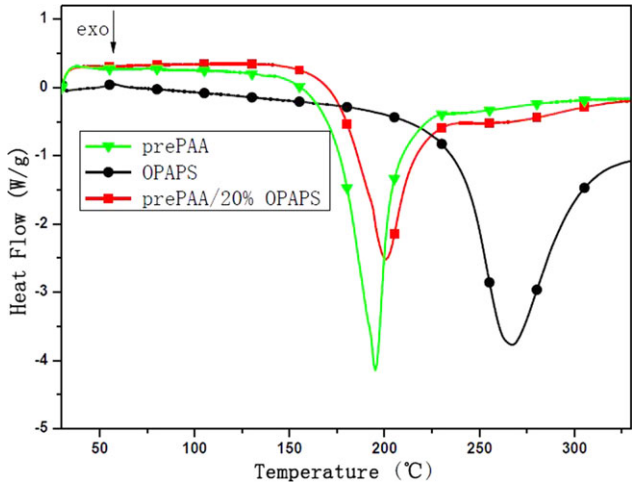

Figure 4. DSC curves of prePAA, OPAPS, and prePAA/20%OPAPS. [Color figure can be viewed in the online issue, which is available at wileyonlinelibrary.com.]

Table II. DSC Results of prePAA and prePAA/20%OPAPS

	Heating rate ϕ (K/min)	5	7.5	10	15
prePAA	ΔH (J/g)	468.4	536.8	513.3	521.1
	T_p (°C)	183.6	189.8	195.1	200.8
	H_p (W/g)	1.73	4.02	4.15	15.6
prePAA/ 20%OPAPS	ΔH (J/g)	342.4	339.5	374.9	434.8
	T_p (°C)	187.9	194.9	200.6	205.5
	H_p (W/g)	1.13	1.74	2.52	5.08

are presented in Table I. FTIR results show that the C—H vibration absorption peaks of —C≡CH (3288 and 610 cm^{-1}) of PAA are significantly weaker compared with those of prePAA. At the same time, the peaks of the C_{Ar}—H stretching vibration (3024 cm^{-1}), the C—H stretching vibration of —CH=CH— (2963 cm^{-1}), the overtone band of the aromatic ring (1900 cm^{-1}), and the C=C stretching vibration (1594 cm^{-1}) appear, obviously due to the formation of the aromatic ring and the conjugated diene structures in the PAA and PAA/OPAPS products. The characteristic peak of the Si—O—Si group at 1102 cm^{-1} appears in PAA/OPAPS composites. In addition, the absorption peak of the —NH— stretching vibration (3374 cm^{-1}) is maintained in the spectra of PAA/OPAPS.

Curing Behaviors of prePAA and prePAA/OPAPS

Figure 4 shows the DSC curves of prePAA, OPAPS, and prePAA/20%OPAPS at the heating rate of 10 K/min. The exothermic peaks in the DSC curves are due to the reaction among the —C≡CH bonds. It is seen that the curing reactions of the C≡CH bonds of OPAPS happen in a wider and higher range of temperatures than that of prePAA, and the temperature of the exothermic peak (T_p) is at 265°C (70°C higher than that of prePAA). The value of T_p of prePAA/20%OPAPS is 5.5°C higher than that of prePAA. At the same time, the exothermal heat (ΔH) (see Table II) of prePAA/20%OPAPS is less than the ΔH of both prePAA and OPAPS because of the incorporation of an inorganic silica-like core into prePAA. This means that prePAA/20%OPAPS has a more controllable curing reaction by copolymerization than prePAA.

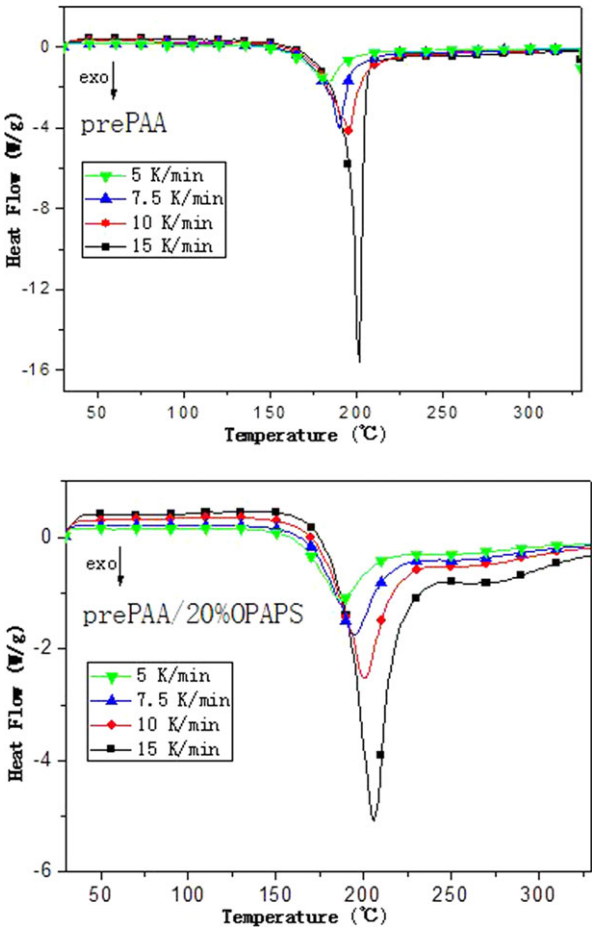

Figure 5. DSC curves of prePAA and prePAA/20%OPAPS at different heating rates. [Color figure can be viewed in the online issue, which is available at wileyonlinelibrary.com.]

The curing kinetics of prePAA and prePAA/20%OPAPS were investigated by DSC measurements in the range of 30−330°C at the heating rates of 5, 7.5, 10, and 15 K/min. Figure 5 shows the curves of heat flow versus the temperature at different heating rates for prePAA and prePAA/20%OPAPS. The exothermal heat ΔH, the temperature of the exothermic peak T_p, and the heat flow at the exothermic peak temperature H_p are listed in Table II.

As shown in Figure 5, the heat-flow curves shifted to higher temperatures as the heating rate increased for the two systems. The average curing reaction heat ΔH is 510 J/g for prePAA but

Table III. Kinetic Parameters of the Thermal Curing Reaction of prePAA and prePAA/20%OPAPS

Samples	Methods	E_a (kJ/mol)	Correlation coefficient R^2	A (10^{11} min^{-1})	n^a
prePAA	Ozawa	108.5	0.9995		0.982
	Kissinger	106.5	0.9994	4.50	
prePAA/ 20%OPAPS	Ozawa	106.2	0.9943		0.978
	Kissinger	103.9	0.9935	1.66	

[a]Crane method.[30]

Applied Polymer SCIENCE

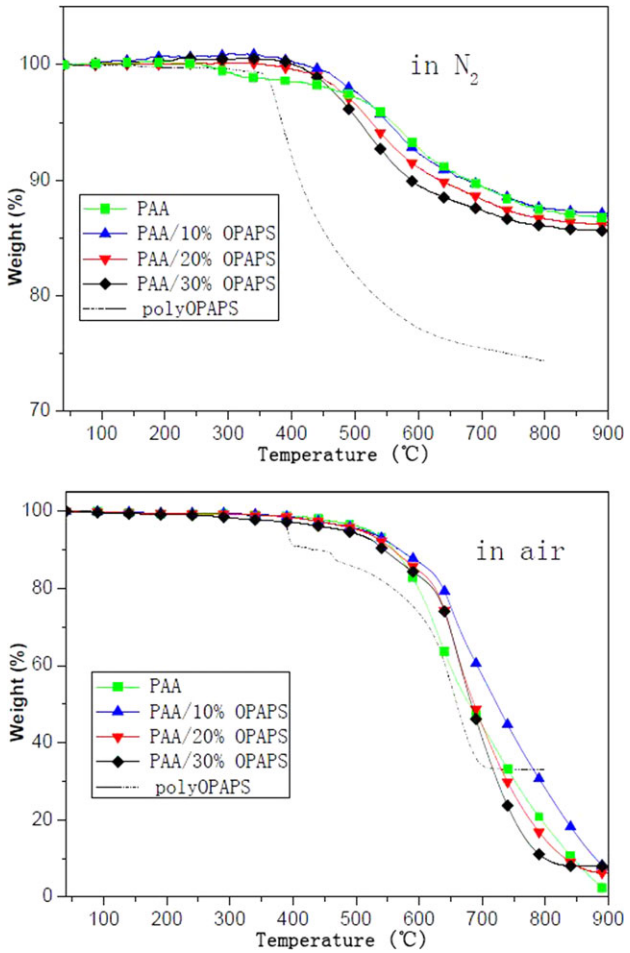

Figure 6. TGA curves of PAA, PAA/OPAPS, and polyOPAPS resins in N_2 and air. [Color figure can be viewed in the online issue, which is available at wileyonlinelibrary.com.]

373 J/g for prePAA/20%OPAPS. Another interesting fact is that the H_p of prePAA is higher than that of prePAA/20%OPAPS, especially at the heating rate of 15 K/min. The low ΔH and H_p of prePAA/20%OPAPS make the curing process easy to control.

The Ozawa and Kissinger methods were used to calculate the kinetic parameters (activation energy E_a, frequency factor A, and reaction order n) of the above-mentioned thermally curing reactions, and the results are shown in Table III.[32–35] The values of E_a calculated according to the Ozawa and Kissinger methods are 108.5 and 106.5 kJ/mol, respectively, for prePAA, and 106.2 and 103.9 kJ/mol, respectively, for prePAA/20%OPAPS. According to our previous work,[26] the values of E_a of OPAPS using the two methods are 133.8 and 122.7 kJ/mol, respectively. The value of E_a of prePAA/20%OPAPS is close to that of prePAA. Furthermore, prePAA shows a much larger frequency factor A compared with prePAA/20%OPAPS in Table III caused by the decrease of the concentration of —C≡CH after adding 20% OPAPS in prePAA, and the large frequency factor A means a large reaction-rate constant.

Thermal Stabilities of PAA and PAA/OPAPS Resins

Resins of PAA and PAA/OPAPS were prepared through a thermal curing program of 130°C/1 h → 150°C/1 h → 170°C/1 h → 190°C/1 h → 210°C/1 h → 230°C/1 h → 250°C/1 h. Their thermal stabilities were evaluated by TGA. A reference polyOPAPS was also prepared by the same curing program. The TGA curves and parameters of these resins in nitrogen and air atmospheres are presented in Figure 6. The relevant thermal decomposition data, including the T_{d1} and T_{d5}, defined as the temperatures at 1 and 5% weight-loss, respectively, and the value of T_{max} defined as the temperatures at the maximum weight-loss rate, and the char residues at 900°C, are given in Table IV.

According to Figure 6, in N_2 atmosphere, PAA/10%OPAPS resin has thermal stability similar to that of PAA resin, but a higher amount of OPAPS seems to be disadvantageous to its thermal stability due to the existence of CH_2 and NH bonds. Nevertheless, in air, PAA/10%OPAPS resin is more resistant to thermal-oxidative degradation than PAA, PAA/20%OPAPS, and PAA/30%OPAPS. Compared with the reference polyOPAPS, OPAPS loading did not change the degradation path of PAA.

PAA and PAA/OPAPS resins were put in the furnace at 1000°C in N_2 for 1 h to obtain their residues. Mass fractions of the residues for PAA, PAA/10%OPAPS, PAA/20%OPAPS, and PAA/30%OPAPS are 83.06%, 82.98%, 76.32%, and 70.09%, respectively. The results are according with the results of TGA. The 10 wt % OPAPS adding to PAA would not destroy the thermal stability of PAA in N_2. The surface of the residue for PAA/30%OPAPS was white, implying a SiO_2 substance. Figure 7 shows the XRD patterns of these residues. The results indicate that the formation of SiO_2 does not improve the thermal stability of PAA/30%OPAPS resins in N_2.

CONCLUSIONS

The curing and thermal properties of prePAA and prePAA/OPAPS hybrids were investigated. The compatibility between

Table IV. TGA Data of PAA, polyOPAPS, and PAA/OPAPS Composites

	In N_2				In air			
	T_{d1} (°C)	T_{d5} (°C)	T_{max} (°C)	Residues (%)	T_{d1} (°C)	T_{d5} (°C)	T_{max} (°C)	Residues (%)
PAA	317.5	558.6	574.0	86.7	332.3	519.8	630.0	1.48
PAA/10%OPAPS	465.1	551.7	572.1	87.2	357.6	512.3	651.9	6.93
PAA/20%OPAPS	441.6	526.0	522.7	86.1	341.0	507.2	651.9	6.29
PAA/30%OPAPS	437.7	507.5	515.7	85.6	216.3	479.8	661.6	8.02
polyOPAPS	361.5	384.0	378.2	74.9	318.1	391.5	657.6	33.1

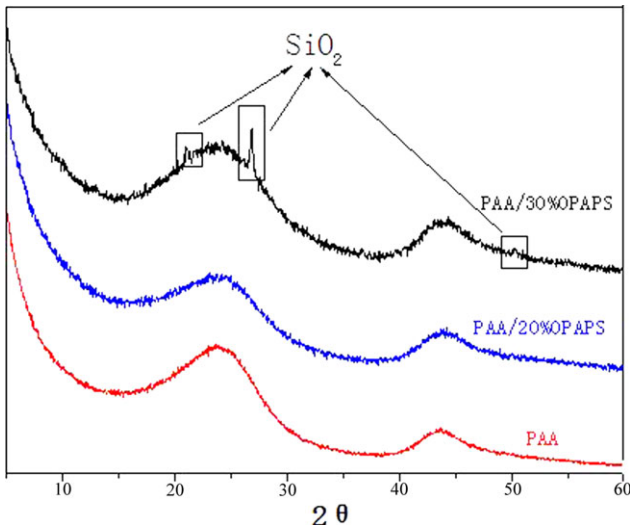

Figure 7. XRD patterns of residues of PAA and PAA/OPAPS resins at 1000°C in N_2 after 1 h. [Color figure can be viewed in the online issue, which is available at wileyonlinelibrary.com.]

prePAA and OPAPS was good due to the reaction of the terminal alkynyl groups between OPAPS and prePAA. FTIR analysis exhibited formation of the conjugated diene and aromatic ring groups in the thermal curing processes of PAA and PAA/OPAPS, and the caged POSS structures were maintained.

The addition of OPAPS to prePAA could decrease the exothermic heat during the cross-linking process of the alkynyl groups. In the DSC curves, prePAA/OPAPS not only showed a higher temperature of the exothermic peak but also wider exothermic ranges and lower exothermal heat than prePAA. These results mean a lower curing rate of prePAA/OPAPS compared with prePAA. Kinetic analysis based on DSC indicates that prePAA and prePAA/OPAPS have the same activation energy, E_a, but different frequency factors, A.

The thermal stabilities of the PAA/OPAPS resins were evaluated. A 10 wt % addition of OPAPS to PAA was able to maintain the excellent thermal stability of PAA in N_2 atmosphere, as evidenced by the mass fraction of residues of the PAA/OPAPS resin heated to 1000°C in N_2 for 1 h, and somewhat enhance the thermal-oxidative stability.

The mechanical properties, especially the ILSS, and the ablative resistance properties of PAA/OPAPS composites need to be studied in the future work.

REFERENCES

1. Katzman, H. A.; Mallon, J. J.; Barry, W. T. *J. Adv. Mater.* **1995**, *4*, 21.
2. Zhang, X. Z.; Huang, Y. D.; Wang, T. Y.; Liu, L. *Compos. Part. A-Appl. S.* **2007**, *38*, 936.
3. Liu, L.; Song, Y. J.; Fu, H. J.; Jiang, Z. X.; Zhang, X. Z. *Appl. Surf. Sci.* **2008**, *254*, 5342.
4. Zaldivar, R. J.; Kobayashi, R. W.; Rellick, G. S. *Carbon.* **1991**, *29*, 1145.
5. Zhang, X. Z.; Huang, Y. D.; Wang, T. Y.; Liu, L. *J. Appl. Polym. Sci.* **2006**, *102*, 5202.
6. Wang, M. C.; Zhao, T. *J. App. Polym. Sci.* **2007**, *105*, 2939.
7. Wang, S. K.; Li, M.; Gu, Y. Z.; Zhang, Z. G. *J. Compos. Mater.* **2010**, *44*, 3017.
8. Yu, L.; Dean, K.; Li, L. *Prog. Polym. Sci.* **2006**, *31*, 576.
9. Zhang, R. L.; Liu, F.; Liu, J. G.; Wang, M. C.; Xia, D. L.; Zhao, T. *Thermosetting Resin.* **2006**, *21*, 1.
10. Luo, Z. H.; Zhao, X. Z.; Zhao, T.; Kuang, S. L. *Polym. Mater. Sci. Eng.* **2011**, *27*, 85.
11. Lickiss, P. D.; Rataboul, F. *Adv. Organomet. Chem.* **2008**, *57*, 1.
12. Cordes, D. B.; Lickiss, P. D.; Rataboul, F. *Chem. Rev.* **2010**, *110*, 2081.
13. Ak, M.; Gacal, B.; Kiskan, B.; Yagci, Y.; Toppare, L. *Polymer.* **2008**, *49*, 2202.
14. Ervithayasuporn, V.; Wang, X.; Gacal, B.; Gacal, B. N. *J. Organomet. Chem.* **2011**, *696*, 2193.
15. Cho, H. S.; Liang, K. W.; Chatterjee, S.; Pittman, C. U. *J. Inorg. Organomet. P.* **2006**, *15*, 541.
16. Liu, H. Z.; Zheng, S. X. *Macromol. Rapid. Commun.* **2005**, *26*, 196.
17. Guo, H. Q.; Meador, M. A.; McCorkle, L. *ACS Appl. Mater. Interfaces.* **2011**, *3*, 546.
18. Zhang, J.; Xu, R. W.; Yu, D. S. *J. Appl. Polym. Sci.* **2007**, *103*, 1004.
19. Ramasundaram, S. P.; Kim, K. J. *Macromol. Symp.* **2007**, *249*, 295.
20. Chou, C. H.; Hsu, S. L.; Dinakaran, K.; Chiu, M. Y.; Wei, K. H. *Macromolecules.* **2005**, *38*, 745.
21. Zhao, Y. Q.; Schiraldi, D. A. *Polymer* **2005**, *46*, 11640.
22. Li, G. Z.; Wang, L. C.; Toghiani, H.; Daulton, T. L.; Koyama, K.; Pittman, C. U. *Macromolecules* **2001**, *34*, 8686.
23. Iyer, S.; Schiraldi, D. A. *Macromolecules* **2007**, *40*, 4942.
24. Franchini, E.; Galy, J.; Gerard, J. F.; Tabuani, D.; Medici, A. *Polym. Degrad. Stab.* **2009**, *49*, 1728.
25. Choi, J.; Kim, S. G.; Laine, R. M. *Macromolecules* **2004**, *37*, 99.
26. Fan, H. B.; He, J. Y.; Yang, R. J. *J. App. Polym. Sci.* **2013**, *127*, 463.
27. Fan, H. B.; Yang, R. J.; Li, D. H. *Acta. Chimica. Sinica.* **2012**, *70*, 429.
28. Fan, H. B.; Yang, R. J.; Li, X. M. *Acta. Chimica. Sinica.* **2012**, *70*, 1737.
29. Fan, H. B.; Yang, R. J. *J. Appl. Polym. Sci.* **2012**, *124*, 4389.
30. Shanmugam, N.; Muthukaruppan, A.; Ian, H. *Acta. Mater.* **2010**, *58*, 3345.
31. Zhang, J.; Xu, R. W.; Yu, D. S. *Eur. Polym. J.* **2007**, *43*, 743.
32. Li, Q.; Zhou, Y.; Huang, X. D.; Deng, S. F.; Huang, F. R.; Du, L.; Li, Z. P. *Eur. Polym. J.* **2008**, *44*, 2538.
33. Zhang, Z. P.; Liang, G. Z.; Ren, P. G.; Wang, J. L. *Polym. Compos.* **2008**, *29*, 77.
34. Hayaty, M.; Beheshty, M. H.; Esfandeh, M. *J. Appl. Polym. Sci.* **2011**, *120*, 62.
35. Dupuy, J.; Leroy, E.; Maazouz, A. *J. Appl. Polym. Sci.* **2000**, *78*, 2262.